Solutions of the axi-symmetric Poisson equation from elliptic integrals. II. Semi-analytical approach

Arnaud Pierens, Jean-Marc Huré

A&A 434, 17–23 (2005)
DOI: 10.1051/0004-6361:20034196

Astronomy & Astrophysics

Solutions of the axi-symmetric Poisson equation from elliptic integrals

II. Semi-analytical approach

A. Pierens[1] and J.-M. Huré[1,2]

[1] LUTh (CNRS UMR 8102), Observatoire de Paris-Meudon, Place Jules Janssen, 92195 Meudon Cedex, France
e-mail: Arnaud.Pierens@obspm.fr
[2] Université Paris 7 Denis Diderot, 2 place Jussieu, 75251 Paris Cedex 05, France
e-mail: Jean-Marc.Hure@obspm.fr

Received 14 August 2003 / Accepted 23 September 2004

Abstract. In a series of two papers, we present numerical integral-based methods to compute accurately the self-gravitating field and potential induced by a tri-dimensional, axially symmetric fluid, with special regard for tori, discs and rings. In this second article, we show that "point mass" singularities are integrable analytically for systems with aspect ratio $(H/R)^2 \ll 1$. We derive second-order accurate, integral formulae for the field components and potential as well, assuming that the mass density locally expands following powers of the altitude (the parabolic case is treated in detail). These formulae are valid inside the entire system: from the equatorial plane to the surface, and especially at the inner and outer edges where they remain regular, in contrast to those derived in the classical bi-dimensional, "razor-thin" approach. Their relative precision $\sim(H/R)^2$ has been checked in many situations by comparison with highly accurate, numerical solutions of the Poisson equation obtained from splitting methods described in Paper I. Time inexpensive and reliable, they offer powerful means to investigate vertically stratified systems where self-gravity plays a role. Three formulae for "one zone" disc models are given.

Key words. gravitation – methods: numerical – methods: analytical

1. Introduction

The construction of simple but fast and reliable tools to properly describe self-gravity in astrophysical discs is of fundamental importance for both modelers and theoreticians. In a first paper (Huré 2005, hereafter Paper I), we have reported general numerical methods to compute accurately the gravity field and potential induced *inside sources* by axially symmetric media, whatever their shape and mass distribution. Purely numerical tools are not always easy to implement, and can be very time-consuming. This can be a severe problem when the Poisson equation is coupled with other equations. On the other hand, there are no reliable algebraic formulae to model the potential and gravity field in discs. Actually, current approximations have a very limited range of application and poor/unknown precision (e.g. Lantian & Xiaoci 1990). For instance, formulae derived without considering the vertical extent as in the "razor-thin" disc approximation (e.g. Binney & Tremaine 1987) do not furnish a full and reliable description of self-gravity (effect of vertical stratification, "appropriate" value for the softening length, etc.). Also, the monopole approximation which assumes that the inner disc is equivalent to a spherical mass distribution (e.g. Mineshige & Umemura 1996, 1997), or the "infinite slab approximation" which neglects radial gradients (Paczynski 1978), not only give incomplete solutions but also simply fail in most situations where self-gravity becomes important.

In this second paper, we propose an intermediate approach between the fully numerical treatment (as considered for instance in Paper I) and simple algebraic formulae which, to our knowledge, do not exist yet. For axially symmetrical, geometrically thin discs (which represent an important family of astrophysical discs), we show that singular kernels in the Poisson integrals can be integrated analytically in the vertical direction, whatever the radial density profile and disc shape (provided the aspect ratio is small). This means i) a considerable gain in terms of computing time since both the field and the potential are obtained from a single quadrature over the radial extent of the system; and ii) regular, well-behaved expressions in particular at the system boundaries. Generic expressions are given assuming that the mass density ρ locally expands in series of the altitude. In Sect. 2, we outline the two major hypotheses of the present calculus. We then derive in Sect. 3 an analytical expression for secondary kernels associated with the field components and potential. In Sect. 4, we consider the special case where the mass density varies quadratically with the altitude

and check the formulae by comparison with highly accurate values obtained using the methods described in Paper I. Three easy-to-use formulae appropriate for "one zone" disc models are given in Sect. 5. Concluding remarks are found in the last section.

2. Assumptions

2.1. Assumption about the aspect ratio

The general idea that underlies the present calculations[1] is based on the Taylor expansion of the modulus k of the complete elliptic integrals (see Eq. (9) in Paper I) with respect to the quantity $u = \frac{z-Z}{a+R}$, where (a, z) are cylindrical coordinates of source points and (R, Z) are coordinates of field points. For $u^2 \ll 1$, we have

$$k^2 = m^2\left(1 - u^2 + \ldots\right) = m^2 + O\left(u^2\right), \tag{1}$$

where m is the characteristic (see Eq. (17) in Paper I), with the consequence that $k \approx m$ at the second-order. Regarding the complementary modulus $k' = \sqrt{1-k^2}$, we have

$$k'^2 = 1 - m^2 + O\left(u^2\right), \tag{2}$$

and so $k'^2 \approx 1 - m^2 = m'^2$. Basically, the condition $u^2 \ll 1$ is fulfilled in two extreme situations:

i) when $\left(\frac{z}{a}\right)^2 \ll 1$ and $|Z| \lesssim |z|$,
ii) when $\left(\frac{Z}{R}\right)^2 \ll 1$ and $|z| \lesssim |Z|$.

The first corresponds to field points located inside systems with moderate/small aspect ratio H/a (namely geometrically thin discs), where H is the semi-thickness. The second situation implies that field points stand close to the mid-plane, whatever the thickness of the system. For geometrically thick discs however, these field points are necessarily located outside (i.e. $R \gg a_{\rm out}$, where $a_{\rm out}$ is the outer radius; see Fig. 2 in Paper I).

2.2. Assumption about the mass distribution

The second hypothesis concerns the mass density $\rho(a, z)$. We assume that it is defined as a finite series[2] of powers of the altitude z, namely

$$\rho(a, z) = \sum_{n=0}^{N} A_n(a)\left(\frac{z}{H}\right)^n, \tag{3}$$

where A_n are positive or negative coefficients, and can depend on the radius a. As in Paper I, the mass density is assumed to vanish at the surface $z = \pm H(a)$, which means certain relations between the $N+1$ coefficients A_n (see for instance Sect. 4). For mathematical reasons, it is preferable to work with an expansion following powers of u, so that Eq. (3) becomes

$$\rho(a, z) = \sum_{n=0}^{N} B_n(a) u^n. \tag{4}$$

Coefficients B_n can be deduced, for each field point, from coefficients A_n from the generic relation

$$B_n = (a+R)^n \sum_{i\geq n}^{N} \frac{A_i}{H^i}\left(\begin{array}{c} i \\ n \end{array}\right) Z^{i-n}, \qquad n = 0, \ldots, N, \tag{5}$$

where $\left(\begin{array}{c} i \\ n \end{array}\right) = \frac{i!}{n!(i-n)!}$ is the binomial coefficent. This relation simplifies into $A_n(a+R)^n = B_n H^n$ at the midplane. Note that B_n depend on a, R, Z and $H(a)$.

3. Field and potential

3.1. The vertical field

Let us start with the exact expression for the secondary kernel associated with the vertical field (see Paper I, Eqs. (8) and (12)) which is the simplest case. We have

$$\breve{\kappa}_Z = \frac{G}{2R\sqrt{aR}} \int_{-H}^{H} \rho(a, z) \frac{k^3 E(k)}{k'^2} (z - Z) \mathrm{d}z. \tag{6}$$

According to Eq. (1), $E(k) \approx E(m)$ at the second-order, and so we can put the complete elliptic integral outside the integral. Using Eq. (4) and changing the order of the operators $\int$ and $\sum$, the general expression for $\breve{\kappa}_Z$ is then

$$\breve{\kappa}_Z \approx \frac{4GaE(m)}{a+R} \sum_{n=0}^{N} B_n(a) I_{n+1}(m'), \tag{7}$$

with

$$I_n(x) = \int_{u^-}^{u^+} \frac{u^n}{x^2 + u^2} \mathrm{d}u, \tag{8}$$

where $u^\pm$ refers to the top/bottom edge of the system, that is

$$u^\pm = \frac{\pm H(a) - Z}{a+R}. \tag{9}$$

We give in the Appendix A the expression of $I_n(x)$ for any $n \geq 0$. Note that the fact that these integrals are defined from a recurrence formula is very convenient in practice. Finally, the vertical gravity field g_Z induced by a disc extending from $a_{\rm in}$ to $a_{\rm out}$ is obtained by integration of Eq. (7) in the radial direction (see Eq. (11) in Paper I), namely

$$g_Z = \int_{a_{\rm in}}^{a_{\rm out}} \breve{\kappa}_Z \mathrm{d}a. \tag{10}$$

Since $\breve{\kappa}_z$ is regular everywhere inside the system provided $\rho(a, \pm H) = 0$ as assumed, g_Z can be computed numerically without difficulty for any field point satisfying $(u^\pm)^2 \ll 1$ for any a. A few examples proving the reliability of this approach are given in Sect. 4.

[1] Background and notations are described in Paper I.

[2] We are confident that such an expansion with $N \neq \infty$ does not necessarily match any arbitrary density profile. In particular, as it is well known, fitting any data sample $\{(z_i, \rho_i)\}_N$ with a high-degree polynomial may become physically irrelevant.

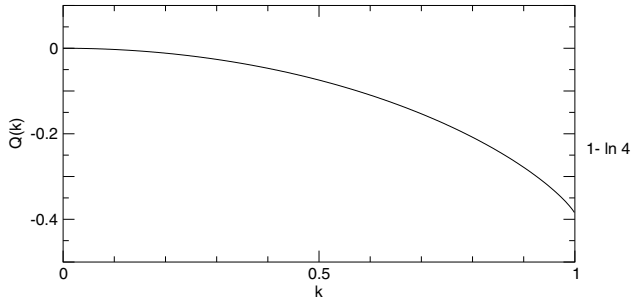

Fig. 1. Function Q versus k.

3.2. The radial field

We shall follow the same approach as above. This case is however a little more tricky because there are two distinct sources of singularity (hyperbolic and logarithmic). The secondary kernel associated with the radial component is (see Paper I, Eqs. (6) and (12))

$$\check{\kappa}_R = \frac{G}{R}\sqrt{\frac{a}{R}} \times \int_{-H}^{H} \rho(a,z) k \left[E(k) - K(k) + \frac{(a-R)k^2 E(k)}{2ak'^2} \right] \mathrm{d}z. \quad (11)$$

As in Paper I, we remove explicitly the logarithmic singularity from the complete elliptic integral of the first kind. Using Eq. (4) and changing the order of the operators as in Sect. 3.1, we then have

$$\check{\kappa}_R \approx 2G\frac{a}{R}\sum_{n=0}^{N} B_n F_n(m'), \quad (12)$$

where $Q(k) = E(k) - K^{\mathrm{reg}}(k)$, K^{reg} being the "regular" elliptic integral of the first kind (see Paper I, Eq. (38) and Fig. 2),

$$F_n(m') = Q(m)J_n + \frac{1}{2}\left[L_n(m') - L_n(1)\right] + \frac{2R(a-R)}{(a+R)^2} E(m) I_n(m'), \quad (13)$$

$$J_n = \int_{u^-}^{u^+} u^n \mathrm{d}u, \quad (14)$$

and

$$L_n(x) = \int_{u^-}^{u^+} u^n \left[\ln\left(x^2 + u^2\right) \right] \mathrm{d}u, \quad (15)$$

where $n \geq 0$. The expressions for J_n and $L_n(x)$ are given in the Appendix A. Like K^{reg}, Q is a weakly varying function in the range $[0, 1]$. It is plotted in Fig. 1. At the second-order in u, $K^{\mathrm{reg}}(k) \approx K^{\mathrm{reg}}(m)$ and $Q(k) \approx Q(m)$. It can be shown that Eq. (12) is never singular and always takes a finite value. The radial field g_R can then be easily determined by integration of $\check{\kappa}_R$, that is (see Paper I, Eq. (11))

$$g_R = \int_{a_{\mathrm{in}}}^{a_{\mathrm{out}}} \check{\kappa}_R \mathrm{d}a. \quad (16)$$

Again, see Sect. 4 for tests.

3.3. The potential

The secondary kernel $\check{\kappa}_\Psi$ associated with the potential Ψ due to an infinitely thin cylinder is (see Paper I, Eqs. (35) and (37))

$$\check{\kappa}_\Psi = -2G\sqrt{\frac{a}{R}} \int_{-H}^{H} \rho(a,z) k K(k) \mathrm{d}z. \quad (17)$$

This term has already been computed in Sect. 3.2. We finally find

$$\check{\kappa}_\Psi \approx -4Ga \sum_{n=0}^{N} B_n P_n(m), \quad (18)$$

where

$$P_n(m) = K^{\mathrm{reg}}(m) J_n - \frac{1}{2}[L_n(m') - L_n(1)]. \quad (19)$$

The integration of $\check{\kappa}_\Psi$ in the radial direction

$$\Psi = \int_{a_{\mathrm{in}}}^{a_{\mathrm{out}}} \check{\kappa}_\Psi \mathrm{d}a \quad (20)$$

yields the potential Ψ. Again, $\check{\kappa}_\Psi$ being regular everywhere, this operation can easily be performed.

4. The parabolic case

4.1. Formulae

With $N = 2$, the mass density in the disc varies quadratically with the altitude. This case is particularly interesting for disc modelers since vertically isothermal discs have a Gaussian density distribution along z which can be well approximated by a parabola (e.g. Frank et al. 1992). Also, the solution of the plane Lane-Emden equation for vertically self-gravitating discs has a similar shape for most gas polytropic indices (Ibanez & Sigalotti 1984). For a quadratic vertical profile vanishing at the surface, we have $A_1 = 0$ and $A_2 = -A_0$ in Eq. (3), whatever a. It follows that coefficients B_n in Eq. (4) are given by

$$\begin{cases} B_0 = \left(1 - \frac{Z^2}{H^2}\right) A_0 \\ B_1 = -\frac{2Z(a+R)}{H^2} A_0 \\ B_2 = -\left(\frac{a+R}{H}\right)^2 A_0. \end{cases} \quad (21)$$

Under these circumstances, the field components and potential are given by the simple formulae

$$g_R \approx 2G \int_{a_{\mathrm{in}}}^{a_{\mathrm{out}}} \frac{a}{R}\left[B_0 I_1(m') + B_1 I_2(m') + B_2 I_3(m')\right] \mathrm{d}a, \quad (22)$$

$$g_Z \approx 4G \int_{a_{\mathrm{in}}}^{a_{\mathrm{out}}} \frac{aE(m)}{a+R}\left[B_0 F_0(m') + B_1 F_1(m') + B_2 F_2(m')\right] \mathrm{d}a, \quad (23)$$

and

$$\Psi \approx -4G \int_{a_{\mathrm{in}}}^{a_{\mathrm{out}}} a\left[B_0 P_0(m) + B_1 P_1(m) + B_2 P_2(m)\right] \mathrm{d}a, \quad (24)$$

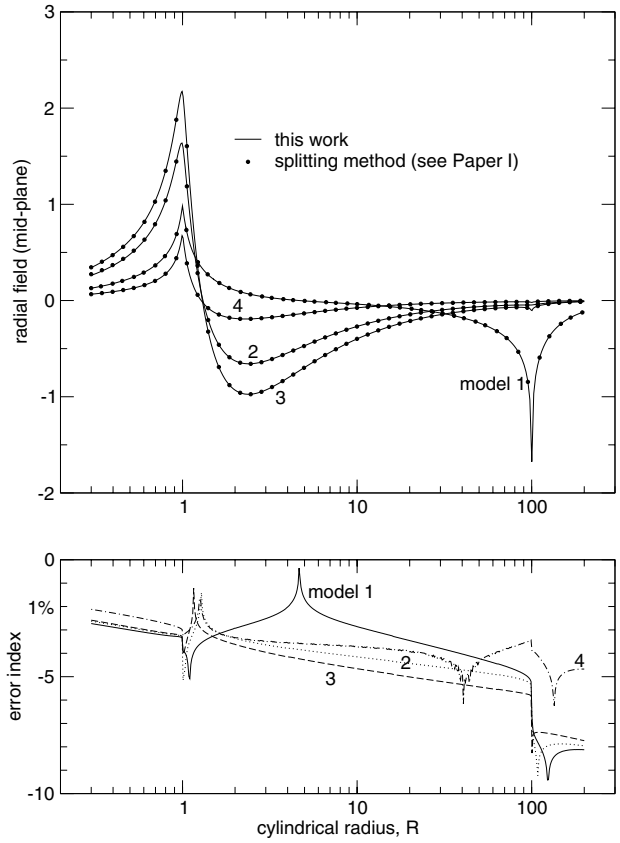

Fig. 2. *Top*: radial field (re-scaled) in the equatorial plane due to a geometrically thin, flared disc with inner edge $a_{\rm in} = 1$ and outer edge $a_{\rm out} = 100$. The mass density varies quadratically with the altitude. Labels 1 to 4 refer to shape and density models listed in Table 1. Two cases are shown: the field is computed from Eq. (22) (*lines*) and compared to highly accurate solutions (*circles*) determined numerically following the density splitting method described in Paper I. *Bottom*: decimal logarithm of the relative error between the two (i.e. the error index). Regions where the error index rises correspond to a vanishing field.

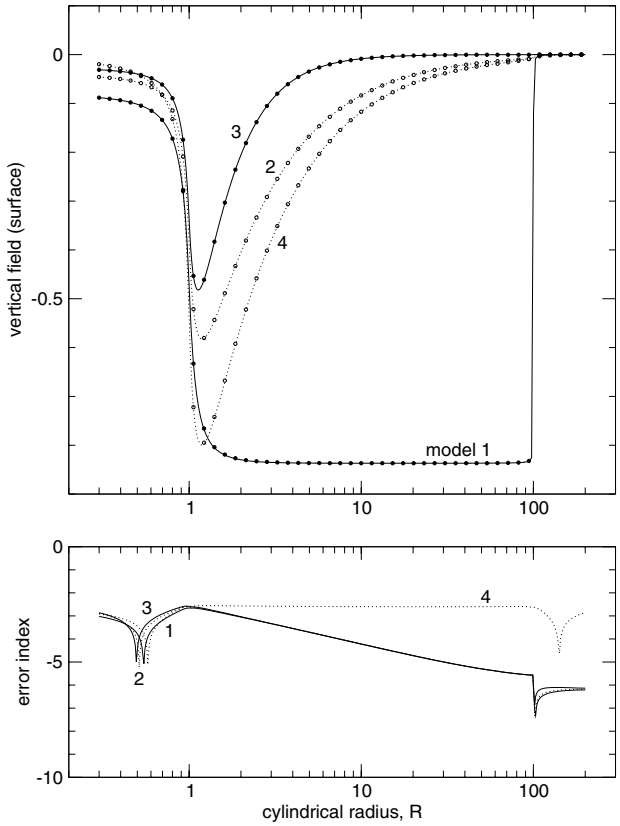

Fig. 3. Same legend and same conditions as for Fig. 2 but for the vertical field component (surface value).

Table 1. Five models for the shape and radial mass density defined to check the reliability of analytical secondary kernels. Model 4 corresponds to a typical astrophysical case: a flared disc with density decreasing outwards. The last model mimics a "jump" (over one scale height) of the density, a situation that can occur in time-dependent simulations. In practice, we take here $H/a_{\rm in} = \frac{1}{10}$, $a_{\rm jump} = \frac{1}{2}(a_{\rm in} + a_{\rm out})$.

Model	Semi-thickness H	Density ρ
1	const.	uniform
2	const.	$\propto a^{-1}$
3	const.	$\propto a^{-2}$
4	$\propto a$	$\propto a^{-2}$
5	$\propto a$	$\propto \frac{1}{a^2}\left[2 + \tanh\frac{a-a_{\rm jump}}{H}\right]$

respectively. Note that neither the shape of the system nor the a-variation of the mass density have yet been specified at this level. The shape $H(a)$ appears in the integral bounds $u^{\pm}$ as well as in coefficients B_n, whereas the function $\rho(a)$ is assigned in the coefficient A_0 only. Thus, Eqs. (22), (23) and (24) are still quite general. As we shall show below, these are second-order accurate. According to the condition on u (see Sect. 2.1), they are valid inside the entire system provided

$$\left(\frac{H(a)-Z}{a+R}\right)^2 \ll 1, \tag{25}$$

for any $a \in [a_{\rm in}, a_{\rm out}]$.

4.2. Examples

Figure 2 shows the mid-plane radial field computed from Eq. (22) and compared to reference values $g_R^{\rm ref.}$ determined following the numerical method described in Paper I. The decimal logarithm of the relative deviation between the two (called the "error index" in Paper I, see Eq. (28)) is also plotted. Here, we have considered a disc extending from $a_{\rm in} = 1$ to $a_{\rm out} = 100$ with shapes and radial density profiles listed in Table 1. We see that, in all models 1 to 4, approximations for the secondary kernels are very good. The relative error is less than $(H/a)^2$, as expected from the order of the k-expansion. Figures 3 and 4 display results obtained for the surface vertical field and mid-plane potential under the same conditions. The same conclusions hold. Finally, Fig. 5 gives the results obtained for model 5 (see Table 1) which corresponds to a flat disc with a density "jump" in the middle. This case can be met for instance in time-dependent simulations if density waves propagate or shocks are

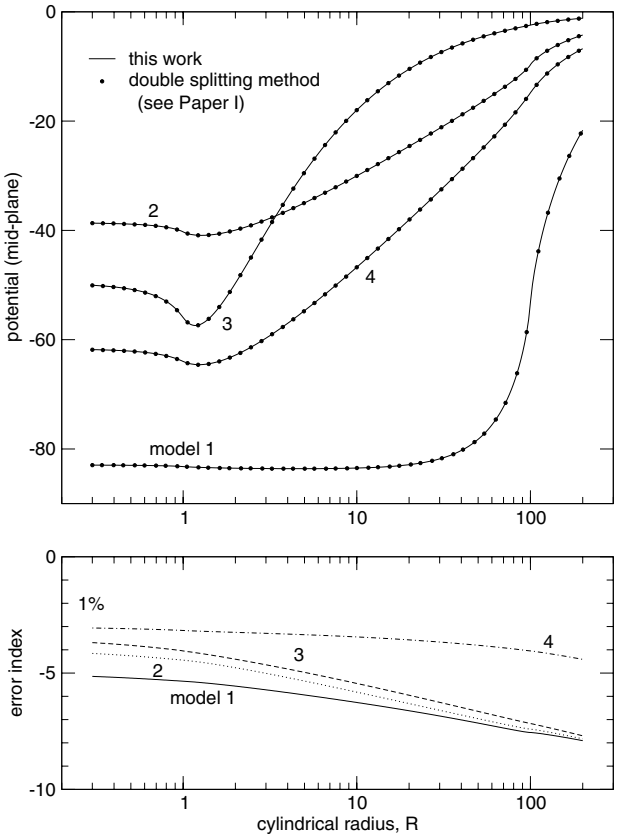

Fig. 4. Same legend and same conditions as for Fig. 2 but for the mid-plane potential.

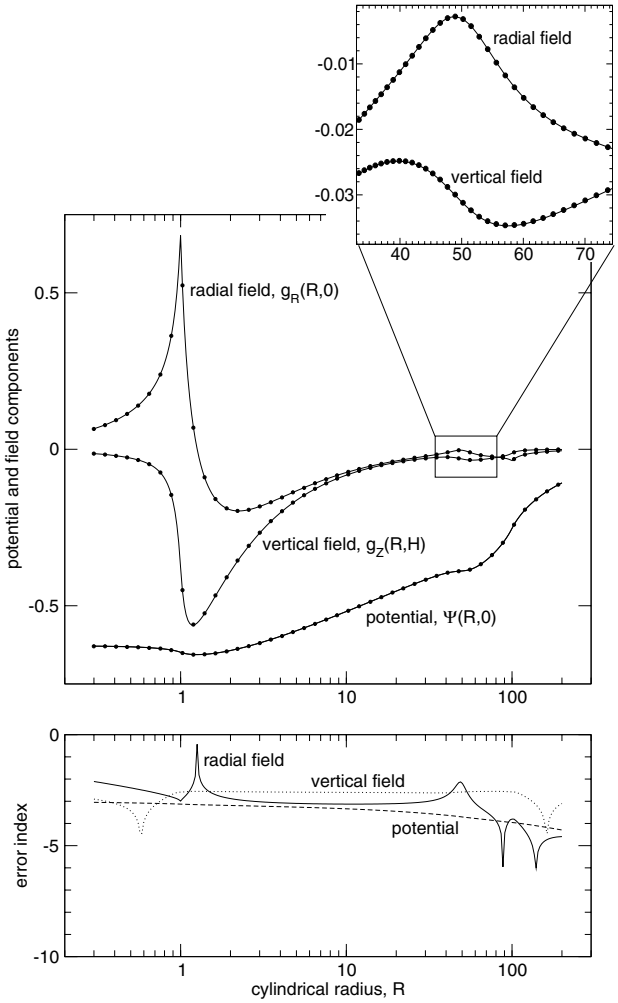

Fig. 5. Same legend and same conditions as for Figs. 2 to 4 but for model 5 (see Table 1). This case corresponds to a density jump at $a_{\rm jump} = 50$ with width $\sim H$.

present in the medium. Again, the analytical approach appears very good, and with the expected accuracy.

We have checked the reliability of our formulae in many other cases and for $N \geq 2$ and our treatment appears indeed reliable. For very large values of N (say larger than 10), a special care must be taken in the numerical implementation. The reason is that coefficients B_n can be large while integrals I_n, J_n and L_n take tiny values. Further, we recommend the use of an adaptive mesh (as in Paper I; see Sect. 4.1), in order to perform efficiently radial quadratures in Eqs. (10), (16) and (20) since integrands remain peaked around field points.

5. Surface and equatorial values: The case for "one-zone" disc models

In "one-zone" disc models (Pringle 1981), physical quantities are currently known at two key-altitudes: the surface and the mid-plane. Regarding hydrostatic equilibrium, vertical gravity is requested at the disc surface. For dynamical equilibrium, radial gravity (and potential) is rather needed at the mid-plane. Integral expressions given before are valid at any altitude Z, and in particular at these two places where they simplify considerably. After rearrangement, we finally find[3]

$$g_Z(R,h) \approx -4G\int_{a_{\rm in}}^{a_{\rm out}} \frac{a\rho_0 E(m)}{a+R}\left\{\frac{2h}{H} - \frac{1}{2}\left[1+\frac{(a-R)^2}{H^2}-\frac{h^2}{H^2}\right]\ln\frac{(a-R)^2+(H-h)^2}{(a-R)^2+(H+h)^2} - \frac{2h(a-R)}{H^2}\left(\mathrm{atan}\,\frac{H-h}{a-R}+\mathrm{atan}\,\frac{H+h}{a-R}\right)\right\}\mathrm{d}a, \quad (26)$$

$$g_R(R,0) \approx 2G\int_{a_{\rm in}}^{a_{\rm out}} \frac{a\rho_0 H}{R(a+R)}\left[2Q(m) + 4\frac{R}{H}E(m)\mathrm{atan}\,\frac{H}{a-R}+\ln\frac{(a-R)^2+H^2}{(a+R)^2+H^2}\right]\mathrm{d}a \quad (27)$$

[3] Expressions (27) and (28) have been obtained in the case $N = 0$, i.e. uniform density in the vertical direction. For geometrically thin discs, variations with the altitude remain small and Eqs. (27) and (28) should be sufficient. If necessary, the reader can derive the full expressions in the case $N = 2$, but these are much bigger.

and

$$\Psi(R,0) \approx -4G\int_{a_{\rm in}}^{a_{\rm out}} \frac{a\rho_0 H}{a+R}\left[-\ln\frac{(a-R)^2+H^2}{(a+R)^2+H^2} +2K^{\rm reg.}(m) -2(a-R)\mathrm{atan}\frac{H}{a-R}+2(a+R)\mathrm{atan}\frac{H}{a+R}\right]\mathrm{d}a \quad (28)$$

where h denote the disc semi-thickness at the field point, i.e. $h = H(R)$. Note that good approximations for $E(m)$, $Q(m)$ and $K^{\rm reg.}(m)$ instead of "exact" values should be sufficient for most astrophysical applications, given the precision of Eqs. (26) to (28). According to Abramowitz & Stegun (1964), we can take

$$E(m) \approx 1 + 0.4630151m'^2 + 0.1077812m'^4 - \left(0.2452727 + 0.0412496m'^2\right)m'^2\ln m'^2, \quad (29)$$

$$K^{\rm reg.}(m) \approx 1.3862944 + 0.1119723m'^2 + 0.0725296m'^4 - \left(0.1213478 + 0.0288729m'^2\right)m'^2\ln m'^2 \quad (30)$$

and

$$Q(m) \approx -0.3862944 + 0.3510428m'^2 + 0.0352516m'^4 - \left(0.1239249 + 0.00123767m'^2\right)m'^2\ln m'^2 \quad (31)$$

which have a precision of $\sim 10^{-5}$.

6. Concluding remarks

In this article, we have derived second-order accurate, integral expressions for the field components and potential, in the case of systems with small to moderate aspect ratio. These formulae are valid inside the system as a whole (and even outside provided $u^2 \ll 1$): from the mid-plane to the surface, and especially at the edge where other approximations generally fail to reproduce the correct behavior of the field and potential. This means that these formulae can be used to self-consistently model vertically averaged discs (e.g. Cannizzo & Reiff 1992) as well as vertically stratified discs (e.g. Cannizzo 1992; D'Alessio et al. 1998; Huré 2000) when prone to self-gravity. Because formally correct for $N \to \infty$ (even if this is not the case in practice), these relations are well suited to various kinds of theoretical problems (stability analysis, etc.).

Although the precision reached here (i.e. H^2/a^2 in relative) should be sufficient for many applications, it is possible to increase the accuracy of the secondary kernels by expanding the modulus to orders higher than 2 (the case considered here). Note that this would imply the expansion of elliptic integrals to equivalent orders, meaning a treatment probably more complex than the one presented here, but this is feasible.

The formulae derived here are expected to fail for $u \gtrsim 0.3$ (corresponding to $u^2 \gtrsim 10\%$). A priori, this means that discs with aspect ratios $H/2a \gtrsim 0.3$ are out of range. However, our formulae continue to be quite satisfactory for aspect ratios much larger than the above limit. This is illustrated in Fig. 6 which displays the potential (and error index) computed from Eq. (24) at the surface, at the midplane and in between, for a system with $H/a = 1$ (model 4 in Table 1). In this example, the potential is good within less than 10% everywhere. Thus, the present approach which is well suited to geometrically thin discs can be applied to geometrically thick discs, but with some caution and within reasonable limits.

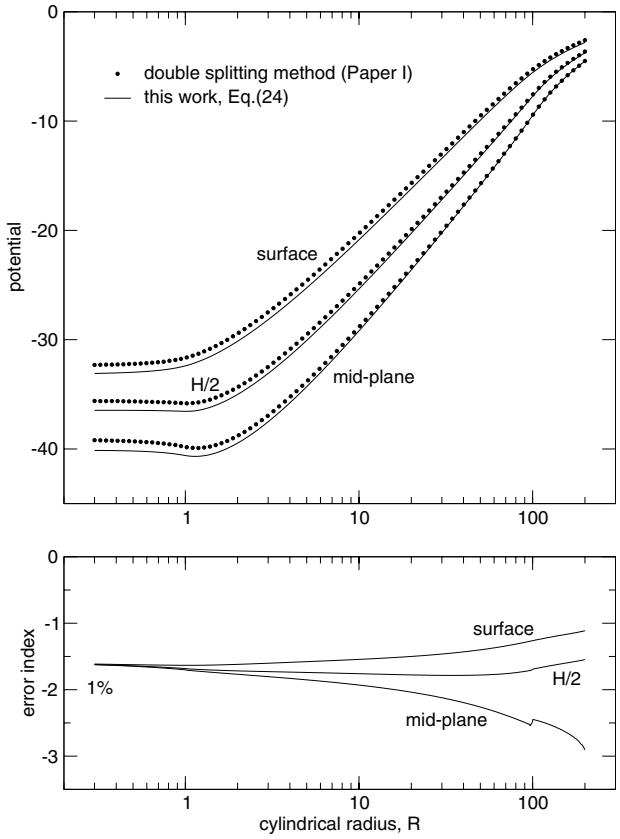

Fig. 6. Same legend and same conditions as for Fig. 4 (model 4) except that the flared disc is geometrically thick with $\frac{H}{a} = 1$. The potential and the error index are given at the mid-plane, at the surface as well as in between (i.e. $Z = H/2$). Curves for the potential have been slightly shifted up and down by a factor of 10% for clarity.

Acknowledgements. We thank D. Pelat for comments on some mathematical points.

Appendix A: Useful formulae

Integral $I_n(x)$ as defined by Eq. (8) is (see for instance Gradshteyn & Ryzhik 1994):

$$I_n(x) = \left[\frac{u^{n-1}}{n-1}\right]_{u^-}^{u^+} - x^2 I_{n-2}(x) \qquad \text{for } n \geq 2, \quad (A.1)$$

$$I_n(x) = \frac{1}{2}\left[\ln\left(x^2+u^2\right)\right]_{u^-}^{u^+} \qquad \text{for } n = 1, \quad (A.2)$$

$$xI_0(x) = \left[\mathrm{atan}\frac{u}{x}\right]_{u^-}^{u^+} \qquad \text{for } n = 0, x \neq 0, \quad (A.3)$$

and

$$I_0(x) = -\left[\frac{1}{u}\right]_{u^-}^{u^+} \qquad \text{for } n = 0, x = 0. \quad (A.4)$$

Integral $J_n(x)$ (see Eq. (14)) is

$$J_n = \begin{cases} [\ln|u|]_{u^-}^{u^+} & n = -1, \\ \left[\frac{u^{n+1}}{n+1}\right]_{u^-}^{u^+} & \text{otherwise.} \end{cases} \quad (A.5)$$

and integral $L_n(x)$ (see Eq. (15)) is

$$L_{2n}(x) = \frac{1}{2n+1}\left[u^{2n+1}\ln\left(x^2+u^2\right) + 2(-1)^n x^{2n+1}\mathrm{atan}\,\frac{u}{x} - 2\sum_{k=0}^{n}\frac{(-1)^{n-k}}{2k+1}x^{2n-2k}u^{2k+1}\right]_{u^-}^{u^+}, \quad (A.6)$$

for even values of n, and

$$L_{2n+1}(x) = \frac{1}{2n+2}\left[\left(u^{2n+2}+(-1)^n x^{2n+2}\right)\ln(x^2+u^2) + \sum_{k=1}^{n+1}\frac{(-1)^{n-k}}{k}x^{2n-2k+2}u^{2k}\right]_{u^-}^{u^+} \quad (A.7)$$

otherwise.

References

Abramowitz, M., & Stegun, I. A. 1964, in Handbook of mathematical functions with examples, graphs and mathematical tables, NBS, Sect. 17

Cannizzo, J. K. 1992, ApJ, 385, 94

Cannizzo, J. K., & Reiff, C. M. 1992, ApJ, 385, 87

D'Alessio, P., Canto, J., Calvet, N., & Lizano, S. 1998, ApJ, 500, 411

Frank, J., King, A., & Raine, D. 1992, in Accretion power in astrophysics, 2nd ed. (Cambridge Uni. Press)

Gradshteyn, I. S., & Ryzhik, I. M. 1994, in Table of integrals, series and products, ed. A. Jeffrey (Academic Press Inc.), 5th ed.

Huré, J.-M. 2000, A&A, 358, 378

Huré, J.-M. 2005, A&A, 434, 1 (Paper I)

Ibanez, S. M. H., & Sigalotti, L. D. 1984, ApJ, 285, 784

Lantian, Y., & Xiaoci, L. 1990, Ap&SS, 172, 293

Mineshige, S., & Umemura, M. 1997, ApJ, 480, 167

Paczynski, B. 1978, Acta Astron., 28, 91

Pringle, J. E. 1981, ARA&A, 19, 137